Fast Electromigration Stress Analysis Considering Spatial Joule Heating Effects

Mohammadamir Kavousi, Liang Chen, Sheldon X.-D. Tan

Department of Electrical and Computer Engineering,

University of California, Riverside

Outline

- Motivation
- Related works and contributions of this work
- New Temperature-Aware EM immortality check in the post-voiding phase
- fast numerical solution for EM induced stress analysis for multi-segment interconnect trees considering TM effect
  - New temperature-aware ODEs by discretizing the coupled EM-TM PDEs
  - Extended Krylov subspace-based reduction technique
- Results and discussion
- Summary

Long term reliability of VLSI remains a serious concern

- Long-term reliability/aging effects such as NBTI (negative biased temperature instability), HCI (hot carrier injection) and EM (Electromigration) **get worse** as **technology advances**.
- **EM** still remains the **top reliability killer** for copper-based interconnects of current integrated circuits (ICs) in 7 nm technology and below.
- EM can lead to circuit **failure** through metal line **resistance change** and over time may result in shorts or opens. (Void or Hillock).
- It is **critical** to develop **fast** and **more accurate** EM models and less conservative EM sign-off and assessment techniques for more EM-aware design and runtime management

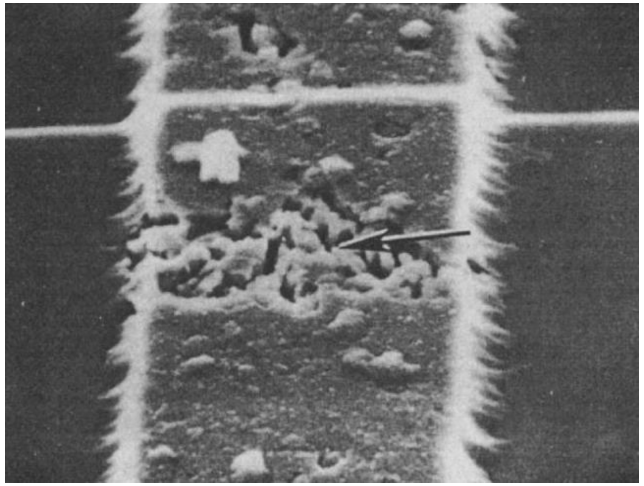

(a)Void

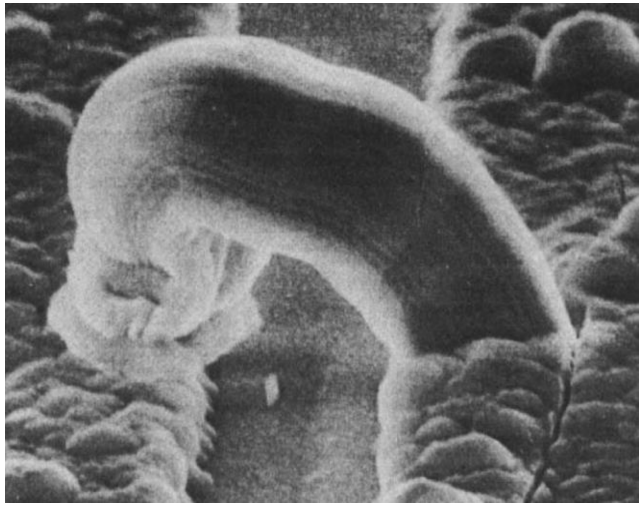

(b)Hillock

The impacts of temperature on EM

- Electromigration (EM) effects
  - Metal migration due to the electrical field, which was well studied and modeled by Korhonen equations
  - Considered to the main driving force for the atom migration
- Thermo-migration (TM) effects
  - Metal atoms will migrate from high temperature to low temperature (so called *Soret Effect*)
  - As a result, the spatial temperature gradients due to Joule heating contribute to the atom migration
  - The effect is **mainly ignored** before and become more announced as technology advances as shown in the right figures.

Electromigration(EM)

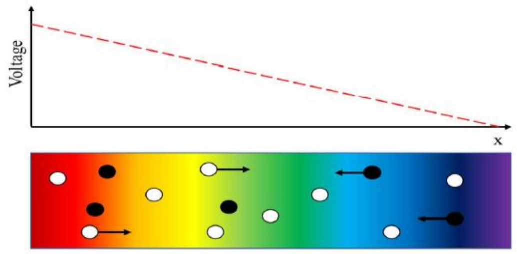

$$J_{EM} = D_v C_v \frac{eZ\rho j}{k_B T}$$

Thermomigration(TM)

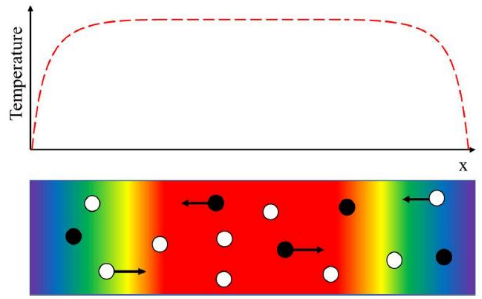

$$J_{TM} = D_v \frac{Q}{k_B T^2} C_v \frac{\partial T}{\partial x}$$

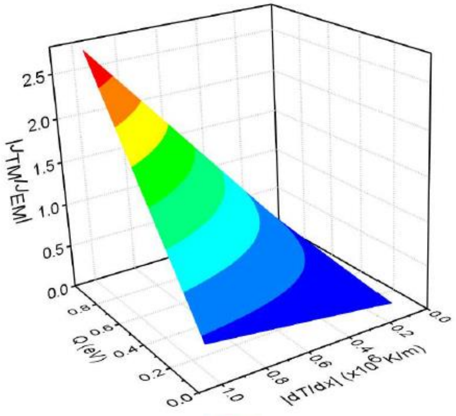

Effect of the heat of transport and temperature gradient on the ratio of TM flux to EM flux, [L. Chen, 2021]

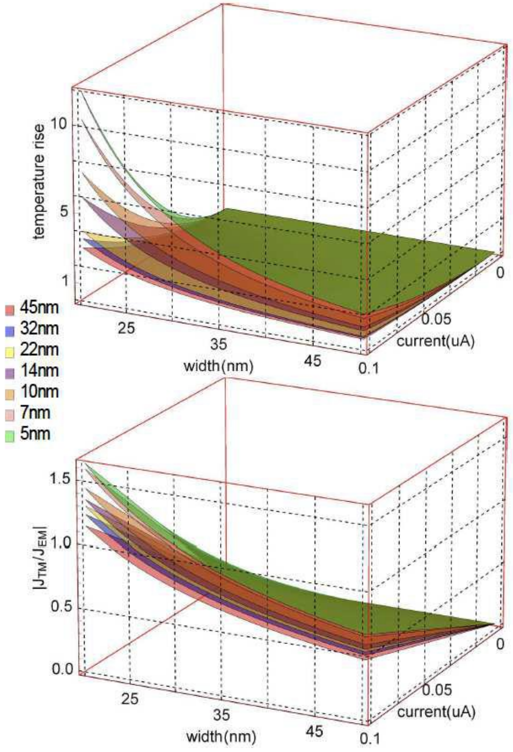

The impact of current, width and technology scaling on (a) temperature rise, (b) the ratio of TM flux to EM flux, for intermediate Interconnect, [Courtesy of Abbasinasab, 2018]

Review of existing work

- Many research works have been proposed recently for physics-based EM analysis but
  - many existing EM methods do not consider thermal effects [1]
  - Some EM analysis research efforts consider transient/temporal thermal effects, but did not consider the spatial temperature or thermal gradient impacts on the multi-segment wires such as FastEM [2]
- Work in [3] investigated spatial temperature impacts on EM.
  - However, the **temperature** of each segment from Joule heating is computed **separately**, which leads to accuracy loss.
- Recently, work in [4] proposed a semi-analytical solutions for transient analysis EM failure process.
  - However, no EM-aware immortality check was studied.

[1] Wentian Jin, Sheriff Sadiqbatcha, Zeyu Sun, Han Zhou, and Sheldon X.-D. Tan. "Em-gan: Data-driven fast stress analysis for multi-segment interconnects", In Proc. IEEE Int. Conf. on Computer Design (ICCD), Oct. 2020.
[2] Chase Cook, Zeyu Sun, Ertugrul Demircan, Mehul D. Shroff, and Sheldon X.-D. Tan. "Fast Electromigration Stress Evolution Analysis for Interconnect Trees Using Krylov Subspace Method", IEEE Trans. on Very Large Scale Integration (VLSI) Systems, May 2018.
[3] A. Abbasinasab and M. MarekSadowska "RAIN:A tool for reliability assessment of interconnect networks—physics to software", IEEE/ACM Design Automation Conference, 2018.
[4] L. Chen, S. X.-D. Tan, Z. Sun, S. Peng, M. Tang and J. Mao, "A Fast Semi-Analytic Approach for Combined Electromigration and Thermomigration Analysis for General Multi-Segment Interconnects", TCAD, 2020.

Contributions

- Joule heat induced temperature are computed for all the wire segments in an interconnect tree, **not** separately.
- we propose a new TM-aware void saturation volume estimation method for fast immortality check in the post-voiding phase.
- We propose a new finite difference method to obtain TM-aware ODEs by discretizing coupled EM-TM equation which is based on Korhonen's equation.
- After discretization, an MOR technique is applied to reduce the size of the original matrices in ODEs and accelerate transient EM stress analysis.

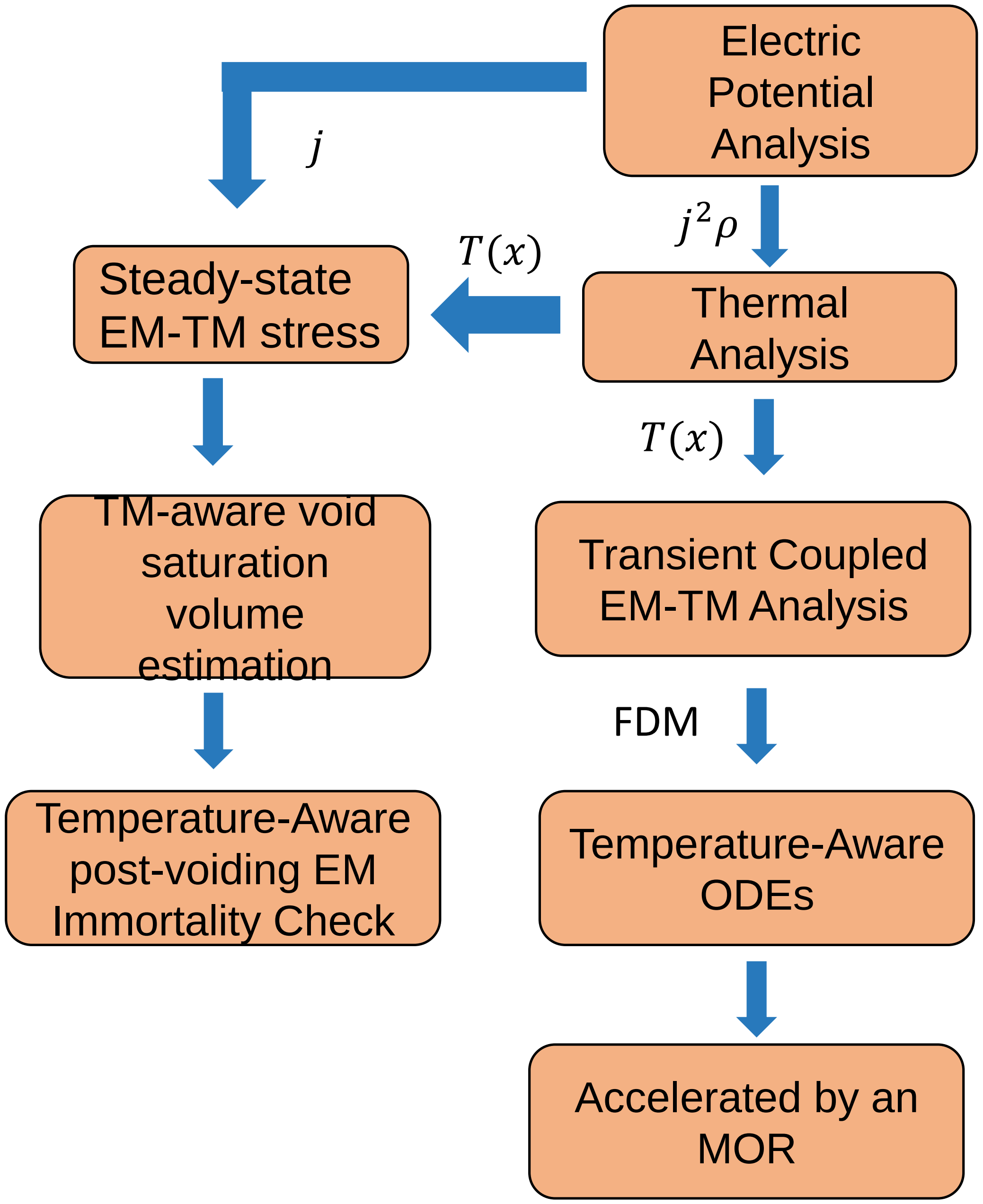

New Saturation-Volume Estimation Considering TM effects

- EM failure process consists of two phases: nucleation, post-voiding phase.
- When the stress reaches the critical value the void is formed and starts to grow, which is the post-voiding phase.
- In the meantime, the boundary conditions at the cathode node (assume x = 0 μm) change, which is given by:

$$\left.\frac{\partial \sigma}{\partial x}\right|_{x=0} = \frac{\sigma(0,t)}{\delta}$$

  - where δ is the effective thickness of the void interface.
- Once the void is formed, the stress at (x = 0 μm) is released to zero.
- Let's define $\sigma_n(x,t)$ $\sigma_p(x,t)$ as the stresses at location x at time t in the nucleation and in the post-voiding phases respectively, then we have:

New Saturation-Volume Estimation Considering TM effects

$$\sigma_p(x,\infty) = \sigma_n(x,\infty) - \sigma_n(0,\infty)$$

- Where $\sigma_n(0,\infty)$ is the pseudo [1] steady-state maximum stress at location x = 0 (the cathode node) for nucleation phase.

- Based on physics we know that the void volu $V_v(t)$ with initial con σ_0 on meets the atom conservation equation:

$$V_v = -\int_{\Omega_L} \frac{\sigma(x,t)}{B} dV + \int_{\Omega_L} \frac{\sigma_0}{B} dV$$

- Where $\sigma(x,t)$ is the stress over time and B sition, is the effective bulk elasticity mod Ω_L s, and is the volume of the remaining interconnect wire.

- In nucleation phase, void siz $V_v(t)$ is always zero since no void is formed.
- Once it enters post-voiding phase, the void si $V_v(t)$ starts to grow.
- After all stresses are released, the void reaches saturation volume, which is the steady state of post-voiding phase.

[1] pseudo means void will not form even the critical stress is reached

New Saturation-Volume Estimation Considering TM effects

- Based on previous equation the steady-state saturation volu V_{sat} of void is expressed as:

$$V_{\text{sat}} = -wh\int_0^L \frac{\sigma_p(x,\infty)}{B}dx + wh\int_0^L \frac{\sigma_0}{B}dx$$
$$= -wh\int_0^L \frac{\sigma_n(x,\infty) - \sigma_n(0,\infty)}{B}dx + wh\int_0^L \frac{\sigma_0}{B}dx$$

  - where w, h and L are the width, thickness and length of the wire, respectively.

- By using atom conservation relation in above equation we have:

$$V_{\text{sat}} = \frac{whL\sigma_n(0,\infty)}{B}$$

New Saturation-Volume Estimation Considering TM effects

- To extend one single wire to a general multi-segment interconnect, the total void saturation volume is calculated by:

$$V_{\text{sat, total}}^{T} = \sum_{ij} \frac{w_{ij} h_{ij} L_{ij}}{B} \frac{eZ}{\Omega} (\mathcal{V}_E^T - U_g^T)$$

- When the void is formed in interior junction node, each segment connected with this node has the void. To estimate the void saturation volume for each segment, based on previous slide we need to calculate the integral of the nucleation stress. we know that:

$$\sum_{ij} \int_{x_i}^{x_j} \sigma(x) w_{ij} h_{ij} dx = \sum_{ij} w_{ij} h_{ij} \Big[(\frac{\sigma_i + \sigma_j}{2}) L_{ij} + \frac{Q}{\Omega} \Big(\ln(\frac{T_0 + T_{m,ij}}{\sqrt{T_i T_j}}) L_{ij} + \frac{(T_i + T_j - 2(T_0 + T_{m,ij}))\Gamma}{T_0 + T_{m,ij}} \tanh(\frac{L_{ij}}{2\Gamma}) \Big) \Big]$$

TM-aware EM Immortality Check Considering Void Saturation Volume

- the kth void saturation volume on the segment which has N_k branches is estimated by:

$$
\begin{aligned}
V^T_{\text{sat, k}} = -\frac{1}{B}\sum_{ij}^{N_k} w_{ij}h_{ij}\Bigg[& (\frac{\sigma_i+\sigma_j}{2})L_{ij} \\
& + \frac{Q}{\Omega}\Bigg(\ln(\frac{T_0+T_{m,ij}}{\sqrt{T_iT_j}})L_{ij} \\
& + \frac{(T_i+T_j-2(T_0+T_{m,ij}))\Gamma}{T_0+T_{m,ij}}\tanh(\frac{L_{ij}}{2\Gamma})\Bigg)\Bigg] \\
& + \sum_{ij}^{N_k}\frac{w_{ij}h_{ij}L_{ij}}{B}\frac{eZ}{\Omega}(\mathcal{V}^T_E - U^T_g) \\
& + \sum_{ij}^{N_k}\int_{x_i}^{x_j} w_{ij}h_{ij}\frac{\sigma_0}{B}dx
\end{aligned}
$$

- The relationship between the total saturation volume and the void volumes for each segment satisfies: $V^T_{\text{sat, total}} = \sum_{k=1}^{N_v} V^T_{\text{sat, k}}$
  - Where N_v is the total number of segments which have the void.
- TM-aware EM immortality check considering void saturation volume can be simply given as: $V^T_{\text{sat, k}} < V^T_{\text{sat, crit}}$
  - where $V^T_{\text{sat, crit}}$ is the given critical void volume before resistance change can happen for the wire

Transient Hydrostatic Stress for Nucleation Phase

- A coupled EM-TM equation based on Korhonen's equation is proposed and well-accepted to estimate hydrostatic stress evolution due to EM

$$PDE: \frac{\partial \sigma}{\partial t} = \frac{\partial}{\partial x}[\kappa(x)(\frac{\partial \sigma}{\partial x} - S - M)],\ t > 0$$

$$BC: \kappa(x_b)(\left.\frac{\partial \sigma}{\partial x}\right|_{x=x_b} - S - M) = 0,\ 0 < t < t_{nuc}$$

$$IC: \sigma(x, 0) = \sigma_T$$

  - Where $\kappa(x) = D_a(T(x))B\Omega/(k_bT(x))$ is a position-dependent diffusivity due to non-uniform temperature, and $D_a = D_0exp(-E_a/(k_bT(x)))$ is atomic diffusion coefficient. D_0 is a constant and E_a is the EM activation energy. $S = \frac{eZ\rho j}{\Omega}$ is EM flux and $M = \frac{Q}{\Omega T}\frac{\partial T}{\partial x}$ is due to TM flux. x_b represents block terminals and σ_T is the initial thermal-induced residual stress.

Finite Difference Method

- To discretize the equation $(\kappa(x)\sigma'(x))'$ using FDM, we can first apply the chain ru $\kappa(x)\sigma''(x) + \kappa'((x)\sigma'(x)$
- However, our study shows such different scheme leads to large errors. Instead, we discretize the second-order term directly:

$$(\kappa(x)\sigma'(x))' = \frac{\kappa(x+\frac{1}{2}\Delta x)\left(\frac{\sigma(x+\Delta x)-\sigma(x)}{\Delta x}\right)}{\Delta x} - \frac{\kappa(x-\frac{1}{2}\Delta x)\left(\frac{\sigma(x)-\sigma(x-\Delta x)}{\Delta x}\right)}{\Delta x}$$

- As a result, the following Finite-difference method is used to discretize the spatial variable x in the TM-aware Korhonen's PDE:

$$\frac{\partial\sigma}{\partial t} = \frac{\kappa(x+\frac{1}{2}\Delta x)\left(\frac{\sigma(x+\Delta x)-\sigma(x)}{\Delta x} - S(x+\frac{1}{2}\Delta x) - \frac{Q}{\Omega T}\frac{T(x+\Delta x)-T(x)}{\Delta x}\right)}{\Delta x} - \frac{\kappa(x-\frac{1}{2}\Delta x)\left(\frac{\sigma(x)-\sigma(x-\Delta x)}{\Delta x} - S(x-\frac{1}{2}\Delta x) - \frac{Q}{\Omega T}\frac{T(x)-T(x-\Delta x)}{\Delta x}\right)}{\Delta x}$$

- Finally, A first order backward method is used to discretize the variable t.

Finite Difference Method

- For demonstration, a two-segment wire example is used.
- The wire is discretized into five nodes; Two edge boundary nodes, one junction node at the middle of the wire, and two non-boundary nodes.
- Boundary conditions are used during the handling of ghost points in the discretization scheme.
- These ghost points are terms in the finite-difference method that do not correspond to physical points on the wire structures.

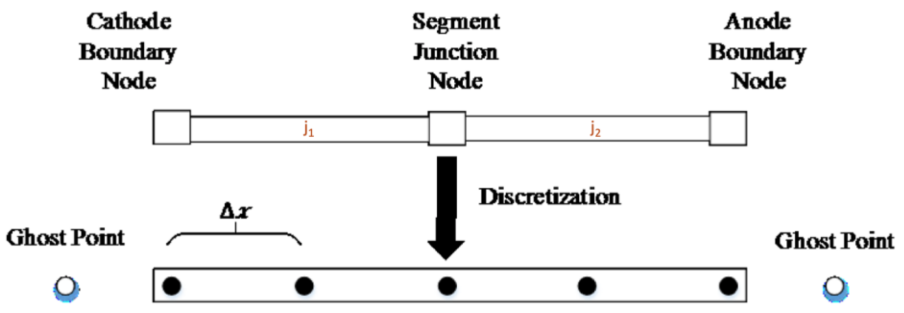

Finite Difference Method

- After some calculations we can create the following LTI ODE dynamic system for nucleation phase:

$$C \begin{bmatrix} \dot{\sigma}_1(t) \\ \dot{\sigma}_2(t) \\ \dot{\sigma}_3(t) \\ \dot{\sigma}_4(t) \\ \dot{\sigma}_5(t) \end{bmatrix} = A \begin{bmatrix} \sigma_1(t) \\ \sigma_2(t) \\ \sigma_3(t) \\ \sigma_4(t) \\ \sigma_5(t) \end{bmatrix} + B \begin{bmatrix} j_1(t) \\ j_2(t) \end{bmatrix} - D$$

$$\sigma(0) = \sigma_T$$

- where C is a 5×5 identity matrix, A,B and D matrices are as follows:

Finite Difference Method for Nucleation Phase

$$A = \begin{bmatrix} -\frac{\kappa(x_1+\frac{\Delta x}{2})}{\Delta x^2} & \frac{\kappa(x_1+\frac{\Delta x}{2})}{\Delta x^2} & 0 & 0 & 0 \\ \frac{\kappa(x_2-\frac{\Delta x}{2})}{\Delta x^2} & -\frac{\kappa(x_2+\frac{\Delta x}{2})-\kappa(x_2-\frac{\Delta x}{2})}{\Delta x^2} & \frac{\kappa(x_2+\frac{\Delta x}{2})}{\Delta x^2} & 0 & 0 \\ 0 & \frac{\kappa(x_3-\frac{\Delta x}{2})}{\Delta x^2} & -\frac{\kappa(x_3+\frac{\Delta x}{2})-\kappa(x_3-\frac{\Delta x}{2})}{\Delta x^2} & \frac{\kappa(x_3+\frac{\Delta x}{2})}{\Delta x^2} & 0 \\ 0 & 0 & \frac{\kappa(x_4-\frac{\Delta x}{2})}{\Delta x^2} & -\frac{\kappa(x_4+\frac{\Delta x}{2})-\kappa(x_4-\frac{\Delta x}{2})}{\Delta x^2} & \frac{\kappa(x_4+\frac{\Delta x}{2})}{\Delta x^2} \\ 0 & 0 & 0 & \frac{\kappa(x_5-\frac{\Delta x}{2})}{\Delta x^2} & -\frac{\kappa(x_5-\frac{\Delta x}{2})}{\Delta x^2} \end{bmatrix}$$

$$B = \beta\rho \begin{bmatrix} -\frac{\kappa(x_1+\frac{\Delta x}{2})}{\Delta x} & 0 \\ -\frac{\kappa(x_2+\frac{\Delta x}{2})-\kappa(x_2-\frac{\Delta x}{2})}{\Delta x} & 0 \\ \frac{\kappa(x_3-\frac{\Delta x}{2})}{\Delta x} & -\frac{\kappa(x_3+\frac{\Delta x}{2})}{\Delta x} \\ 0 & -\frac{\kappa(x_4+\frac{\Delta x}{2})-\kappa(x_4-\frac{\Delta x}{2})}{\Delta x} \\ 0 & \frac{\kappa(x_5-\frac{\Delta x}{2})}{\Delta x} \end{bmatrix} \quad D = \begin{bmatrix} -\frac{\kappa(x_1+\frac{\Delta x}{2})M(x_1+\frac{\Delta x}{2})}{\Delta x} \\ -\frac{\kappa(x_2+\frac{\Delta x}{2})M(x_2+\frac{\Delta x}{2})-\kappa(x_2-\frac{\Delta x}{2})M(x_2-\frac{\Delta x}{2})}{\Delta x} \\ -\frac{\kappa(x_3+\frac{\Delta x}{2})M(x_3+\frac{\Delta x}{2})-\kappa(x_3-\frac{\Delta x}{2})M(x_3-\frac{\Delta x}{2})}{\Delta x} \\ -\frac{\kappa(x_4+\frac{\Delta x}{2})M(x_4+\frac{\Delta x}{2})-\kappa(x_4-\frac{\Delta x}{2})M(x_4-\frac{\Delta x}{2})}{\Delta x} \\ \frac{\kappa(x_5-\frac{\Delta x}{2})M(x_5-\frac{\Delta x}{2})}{\Delta x} \end{bmatrix}$$

where $\beta = \frac{eZ}{\Omega}$

Finite Difference Method for Post-voiding Phase

- PDE for post-voiding phase is the same as nucleation phase
- IC is the stress at $t = t_{nuc}$ in the nucleation phase.
- As mentioned before BC in the post-voiding phase is different from nucleation's BC.
- This leads to the following matrices:

$$A = \begin{bmatrix} -\frac{\kappa(x_1+\frac{\Delta x}{2})}{\Delta x^2} - \frac{\kappa(x_1)}{\Delta x \delta} & \frac{\kappa(x_1+\frac{\Delta x}{2})}{\Delta x^2} & 0 & 0 & 0 \\ \frac{\kappa(x_2-\frac{\Delta x}{2})}{\Delta x^2} & -\frac{\kappa(x_2+\frac{\Delta x}{2})-\kappa(x_2-\frac{\Delta x}{2})}{\Delta x^2} & \frac{\kappa(x_2+\frac{\Delta x}{2})}{\Delta x^2} & 0 & 0 \\ 0 & \frac{\kappa(x_3-\frac{\Delta x}{2})}{\Delta x^2} & -\frac{\kappa(x_3+\frac{\Delta x}{2})-\kappa(x_3-\frac{\Delta x}{2})}{\Delta x^2} & \frac{\kappa(x_3+\frac{\Delta x}{2})}{\Delta x^2} & 0 \\ 0 & 0 & \frac{\kappa(x_4-\frac{\Delta x}{2})}{\Delta x^2} & -\frac{\kappa(x_4+\frac{\Delta x}{2})-\kappa(x_4-\frac{\Delta x}{2})}{\Delta x^2} & \frac{\kappa(x_4+\frac{\Delta x}{2})}{\Delta x^2} \\ 0 & 0 & 0 & \frac{\kappa(x_5-\frac{\Delta x}{2})}{\Delta x^2} & -\frac{\kappa(x_5-\frac{\Delta x}{2})}{\Delta x^2} \end{bmatrix}$$

$$B = \beta\rho \begin{bmatrix} 0 & 0 \\ -\frac{\kappa(x_2+\frac{\Delta x}{2})-\kappa(x_2-\frac{\Delta x}{2})}{\Delta x} & 0 \\ \frac{\kappa(x_3-\frac{\Delta x}{2})}{\Delta x} & -\frac{\kappa(x_3+\frac{\Delta x}{2})}{\Delta x} \\ 0 & -\frac{\kappa(x_4+\frac{\Delta x}{2})-\kappa(x_4-\frac{\Delta x}{2})}{\Delta x} \\ 0 & \frac{\kappa(x_5-\frac{\Delta x}{2})}{\Delta x} \end{bmatrix}$$

$$D = \begin{bmatrix} 0 \\ \frac{\kappa(x_2+\frac{\Delta x}{2})M(x_2+\frac{\Delta x}{2})-\kappa(x_2-\frac{\Delta x}{2})M(x_2-\frac{\Delta x}{2})}{\Delta x} \\ \frac{\kappa(x_3+\frac{\Delta x}{2})M(x_3+\frac{\Delta x}{2})-\kappa(x_3-\frac{\Delta x}{2})M(x_3-\frac{\Delta x}{2})}{\Delta x} \\ \frac{\kappa(x_4+\frac{\Delta x}{2})M(x_4+\frac{\Delta x}{2})-\kappa(x_4-\frac{\Delta x}{2})M(x_4-\frac{\Delta x}{2})}{\Delta x} \\ -\frac{\kappa(x_5-\frac{\Delta x}{2})M(x_5-\frac{\Delta x}{2})}{\Delta x} \end{bmatrix}$$

where $\beta = \frac{eZ}{\Omega}$

Model Order Reduction

- After the stress evolution PDE has been discretized into the ODE , it can be written into the following time-invariant dynamic system:

$$C\dot{\sigma}(t) = A\sigma(t) + Bj(t) - D$$
$$\sigma(0) = [\sigma_1(0), \sigma_2(0), ..., \sigma_n(0)]$$

  - where the stress vector is represented by $\sigma(t)$, $\sigma(0)$ is the initial stress at $t = 0$ due to thermal-mechanical interaction. C, A are $n \times n$ matrices, D is n$\times$ 1 constant matrix for $t > 0$ and B is the n$\times$ p input matrix, where p is the number of inputs or the size of driving current density sources $j(t)$, which can be time-varying and is represented by the piecewise constant waveform: $$j(t) = u_1(t) + u_2(t - t_1) + ... + u_N(t - t_{N-1})$$
  - Above equation can be solved using the Backward Euler method. But this method is slow.
  - First, an MOR technique is applied on abovementioned equation then the Backward Euler method is used to efficiently obtain EM stress.

Model Order Reduction

- This is the matrix A for nucleation phase we already obtained:

$$A = \begin{bmatrix} -\frac{\kappa(x_1+\frac{\Delta x}{2})}{\Delta x^2} & \frac{\kappa(x_1+\frac{\Delta x}{2})}{\Delta x^2} & 0 & 0 & 0 \\ \frac{\kappa(x_2-\frac{\Delta x}{2})}{\Delta x^2} & -\frac{\kappa(x_2+\frac{\Delta x}{2})-\kappa(x_2-\frac{\Delta x}{2})}{\Delta x^2} & \frac{\kappa(x_2+\frac{\Delta x}{2})}{\Delta x^2} & 0 & 0 \\ 0 & \frac{\kappa(x_3-\frac{\Delta x}{2})}{\Delta x^2} & -\frac{\kappa(x_3+\frac{\Delta x}{2})-\kappa(x_3-\frac{\Delta x}{2})}{\Delta x^2} & \frac{\kappa(x_3+\frac{\Delta x}{2})}{\Delta x^2} & 0 \\ 0 & 0 & \frac{\kappa(x_4-\frac{\Delta x}{2})}{\Delta x^2} & -\frac{\kappa(x_4+\frac{\Delta x}{2})-\kappa(x_4-\frac{\Delta x}{2})}{\Delta x^2} & \frac{\kappa(x_4+\frac{\Delta x}{2})}{\Delta x^2} \\ 0 & 0 & 0 & \frac{\kappa(x_5-\frac{\Delta x}{2})}{\Delta x^2} & -\frac{\kappa(x_5-\frac{\Delta x}{2})}{\Delta x^2} \end{bmatrix}$$

- We notice that the determinant of matrix A in the previous ODE is zero and this is a singular matrix for nucleation case, which actually is a known problem and is mitigated in FastEM.
- The reason is that the stress variables for the wire nodes are not independent.
- As mentioned before, from atom conservation we have:

$$\sum_k a_k \sigma_k(t) = \sum_k a_k \sigma_k(0)$$

  - where $\sigma_k(0)$ is initial stress and a_k is the total area of branches.
- Therefore, we can use above equation to replace a dependent row in our ODE, hence the matrix A for nucleation phase becomes an invertible matrix.

Model Order Reduction

- We transform our modified ODE into the frequency domain using the Laplace transformation.
- Notice that D is $n \times 1$ constant matrix for $t > 0$, hence it can be considered as $Du(t)$ where $u(t)$ is the unit step function. Therefore, we have:

$$sC\sigma(s) - C\sigma(0) = A\sigma(s) + \frac{1}{s}(BJ(s) - D)$$

  - where the Laplace transformation of $j(t)$ is computed as: $J(s) = \frac{1}{s}\left(\sum_{i=1}^{N} u_i e^{t_{i-1}}\right) = \frac{1}{s}J$

- Then we follow the similar extended Krylov subspace reduction/simulation method used in [FastEM]. Let $\bar{\sigma}(s) = s\sigma(s) = (m_0 + m_1 s + m_2 s^2 + ...)$, be the moment representation of the unknown responses, above equation can be rewritten as:

$$sC(m_0 + m_1 s + m_2 s^2 + ...) - sC\sigma(0)$$
$$= A(m_0 + m_1 s + m_2 s^2 + ...) + BJ - D$$

Extended Krylov Subspace Model Order Reduction

- Last equation leads to a recursive response moment computation as:

$$
\begin{aligned}
m_0 &= -A^{-1}(BJ - D) \\
m_1 &= A^{-1}C(m_0 - \sigma(0)) \\
m_2 &= A^{-1}Cm_1 \\
&\vdots \\
m_{q-1} &= A^{-1}Cm_{q-2}
\end{aligned}
$$

- For the Krylov subspace method, as shown in Algorithm 1 , an existing modified Arnoldi process [FastEM] is used to compute the orthonormalized response moment space.

Algorithm 1: Modified Arnoldi Method

Result: $V_q = [v_1 \dots v_q]$
$b = -A^{-1}(BJ - D);$
$G = A^{-1}C;$
$v_1 = b/\|b\|_2;$
for $j = 1;\ j <= q;\ j++$ **do**
  if $j == 1$ **then**
    $w = G(v_j - \sigma(0));$
  else
    $w = G(v_j);$
  end
  for $i = 1;\ i <= j;\ i++$ **do**
    $h_{i,j} = w^T v_i;$
    $w = w - h_{i,j} v_i;$
  end
  $h_{j+1,j} = \|w\|_2;$
  if $h_{j+1,j} != 0$ **then**
    $v_{j+1} = w/h_{j+1,j};$
  end
end

Extended Krylov Subspace Model Order Reduction

- Once we obtain the projection matrix V_q , our ODE can be order-reduced using the following matrices:

$$\hat{A} = V_q^T A V_q$$
$$\hat{C} = V_q^T C V_q$$
$$\hat{B} = V_q^T B$$
$$\hat{D} = V_q^T D$$
$$\hat{\sigma}(0) = V_q^T \sigma(0)$$

- Where q is the number of pole in krylov subspace method, $\hat{A}$ and $\hat{C}$ are reduced $q \times q$ matrices, $\hat{B}$ and $\hat{D}$ are the reduced $q \times p$ and $q \times 1$ matrices respectively. $\hat{\sigma}(0)$ is reduced initial condition $q \times 1$ vector.

- Then, the resulting reduced ODE LTI stress evolution system with the initial condition can be written as:

$$\hat{C}\dot{\hat{\sigma}}(t) = \hat{A}\hat{\sigma}(t) + \hat{B}j(t) - \hat{D}$$
$$\hat{\sigma}(0) = [\hat{\sigma}_1(0), \hat{\sigma}_2(0), ..., \hat{\sigma}_n(0)]$$

- Then, transient simulations in the time domain using backward-Euler time integration method can be performed on above reduced ODE, which will be much more efficient to simulate than our original ODE system.

- After the reduced response is obtained, then, the original response can be obtained by: $\sigma(t) = V_q \times \hat{\sigma}(t)$

Saturation Volume Estimation

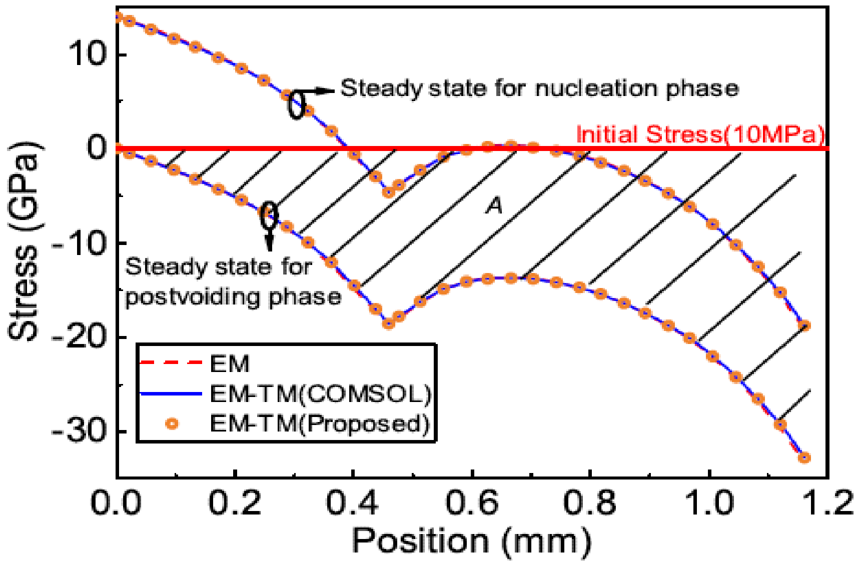

(a)

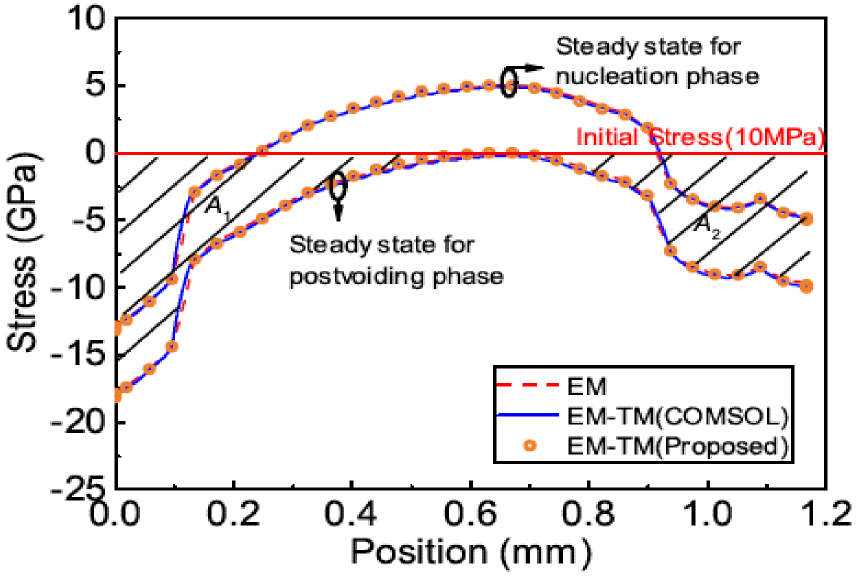

(b)

- Figures shows steady-stress in void nucleation phase and post-voiding phase with (a) terminal void and (b) interior void.
- Once the void is formed, the maximum stress is released to zero; After that, interconnect in Fig. (b) is divided into two sub-wires. By calculating areas A1 and A2, we can estimate the saturation volume of two sub-wires separately.

Saturation Volume Estimation

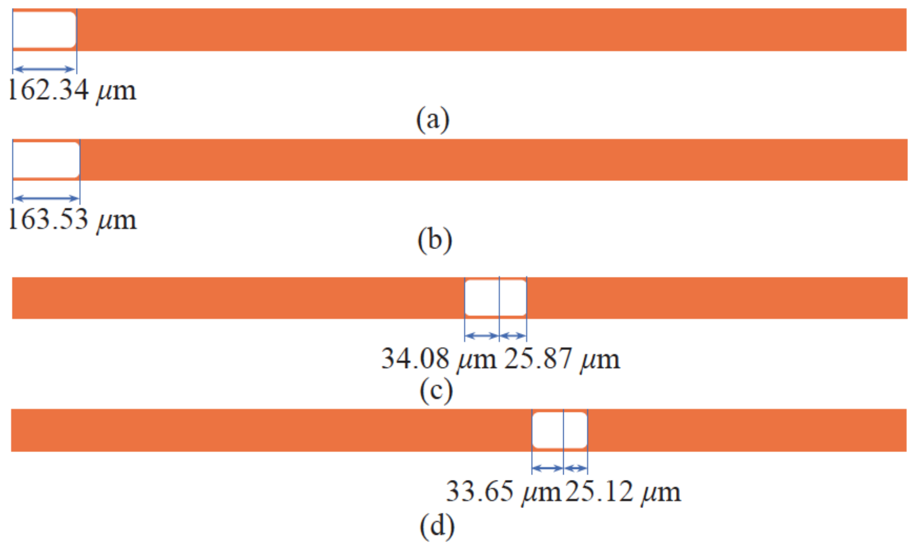

- The length of voids for (a) TM-aware and (b) EM saturation volume estimation for the first example with terminal void. The length of voids for (c) TM-aware and (d) EM saturation volume estimation for the second example with interior void. In the second example, the maximum stress is placed at the mid part of the straight-line multi-segment interconnect, both location and size of the voids for TM-aware and EM immortality check are different.

	EM(μm^3)		EM-TM(μm^3)				Rel. Err. (%)
			COMSOL		Proposed		
1	64.756		64.291		64.286		0.008
2	3.461	2.584	3.507	2.662	3.505	2.661	0.049

- From two examples, considering Joule heating effects is very important for the accurate prediction of EM reliability.
- To validate the accuracy of the analytical solution, commercial software COMSOL is also employed to calculate the saturation volume. As shown in the Table, the analytical results agree well with that of

Transient Hydrostatic Stress Analysis Using the Proposed FDM

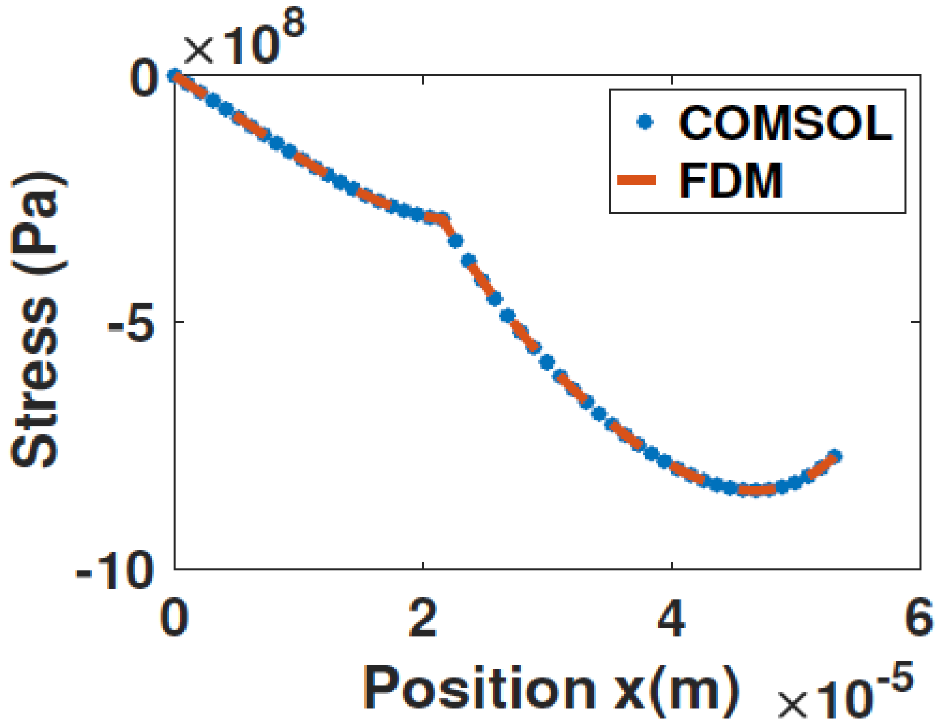

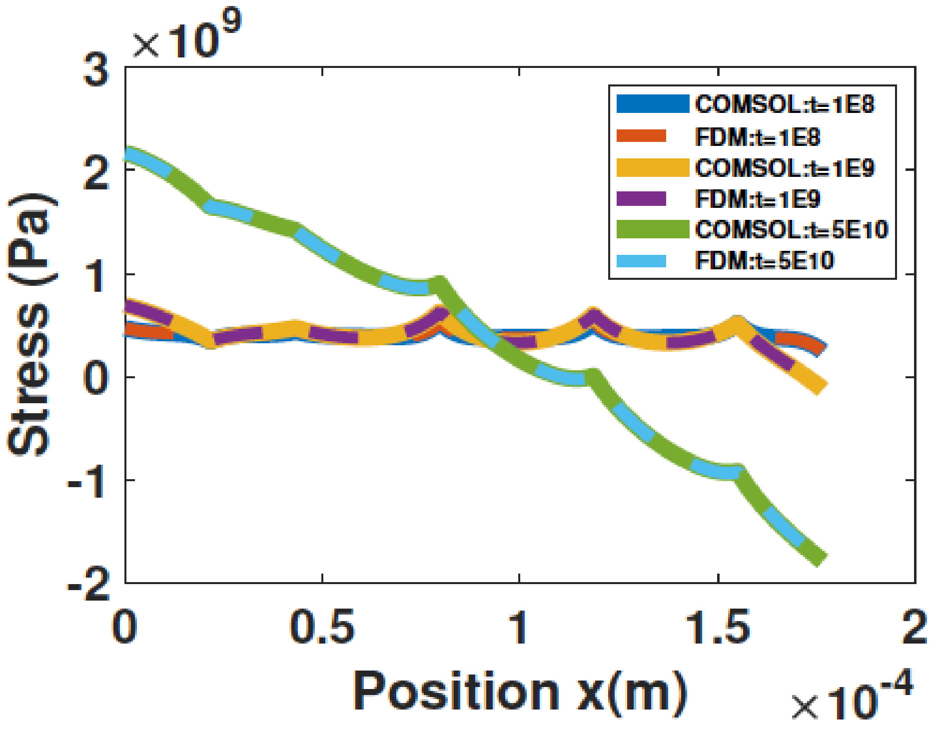

Growth stage validation for two wire segments at $t = 1E9$

Nucleation stage validation for nine segments wire.

Transient Hydrostatic Stress Analysis Using MOR

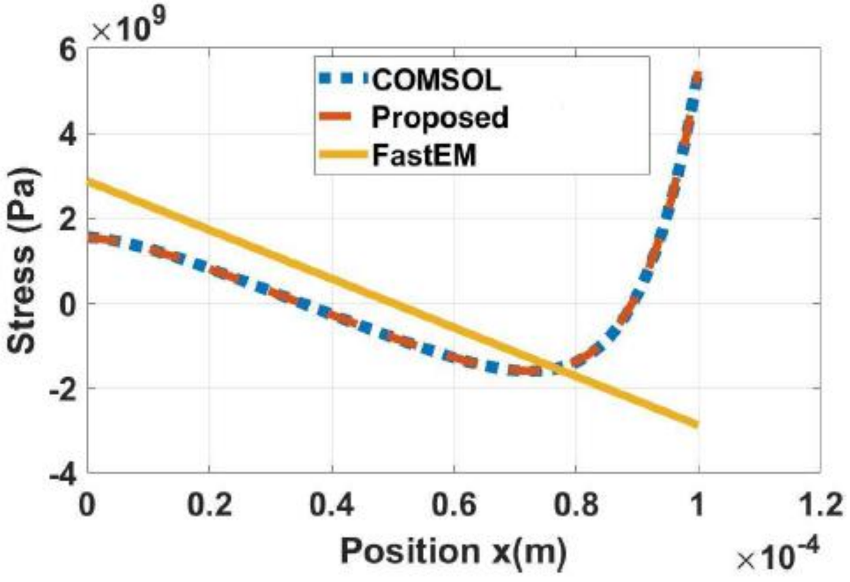

Steady-state stress comparison between the new method, [FastEM] and COMSOL.

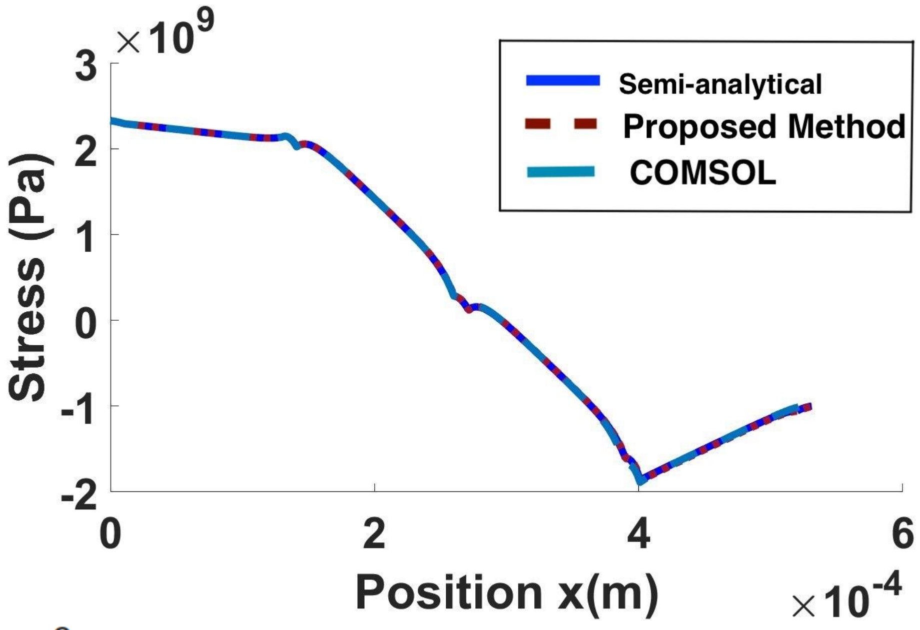

Steady-state stress comparison between the proposed method and the semi-analytical state of the art method proposed by L. Chen et al. (2020)

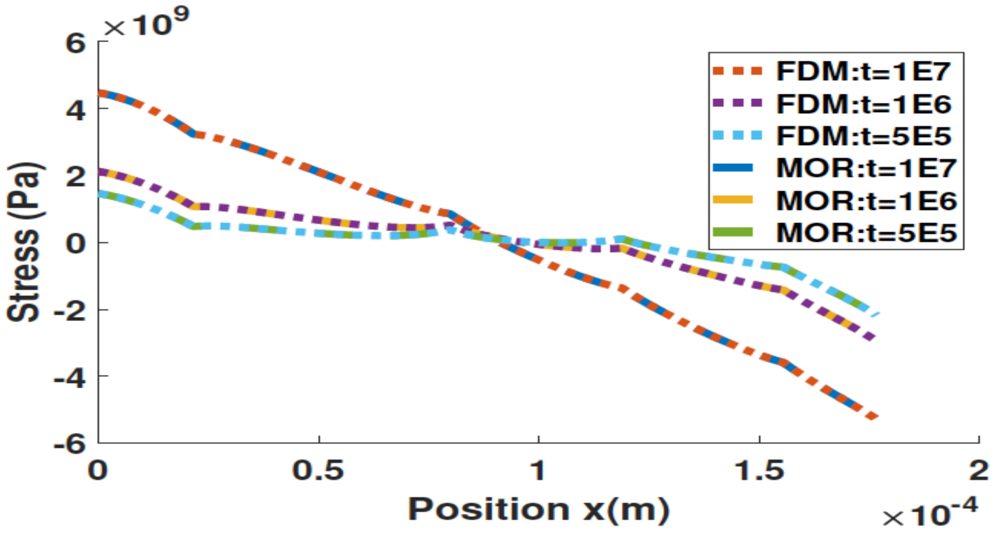

MOR validation for 6 wire segments with q=5.

Transient Hydrostatic Stress Analysis Using MOR

$\#branch$	Method by Chen (s)	New TM-EM (s)	Speed-up
20	6.4451	0.0469	137.42×
50	16.3721	0.4681	34.98×
100	35.2561	1.3651	25.83×
200	83.5570	6.7356	12.41×
400	224.0334	40.5487	5.53×
500	324.1820	72.3226	4.48×
700	604.5640	190.4173	3.17×
1000	1307.7429	572.2694	2.29×

- The Table shows the performance comparison between our proposed MOR-accelerated TM-EM analysis method and recently proposed TM-aware EM analysis by L. Chen et al. (2020)
- As we can see, the proposed MOR-accelerated method can achieve about 28 × speedup on average for all the examples in this table.

Summary

- A new analytic **TM-aware** void **saturation volume** estimation formula for fast EM **immortality check** was proposed.
- A **fast** numerical frequency domain analysis techniques for solving **TM-aware** partial differential equations for both nucleation and post-voiding phases were presented.
- Numerical results showed that compared to the **COMSOL**, our proposed **temperature-aware** immortality check are much **more accurate** than recently proposed methods.
- Also the results show that our proposed TM-aware transient EM stress solution is 28 × **faster** than recently proposed method, on average for the interconnect with up to 1000 branches, which cover the majority of typically power grid networks.

Thank You!

Questions???